Electronic supplementary information (ESI)

A feasible strategy of coating $CoMoO_4$ on $Co_{11}(HPO_3)_8(OH)_6$ nanorods for improved practical application in supercapacitors

Wei Guo[a], Tao Yang[b], Lianjie Huang[b], Wei Hou[b], Shuang Wang[b,c,*]

a. College of Physics and Optoelectronics, Taiyuan University of Technology, Jinzhong, 030060, P.R. China;

b. College of Environmental Science and Engineering, Taiyuan University of Technology, Jinzhong, 030600, P.R. China;

c. Shanxi Key Laboratory of Gas Energy Efficient and Clean Utilization, Taiyuan University of Technology, Taiyuan, 030024, P.R. China.

[*]Corresponding author.
E-Mail address: wangshuang@tyut.edu.cn (S. Wang)

1. Experimental section

1.1 Materials

Sodium hypophosphite ($NaH_2PO_2·H_2O$, 99%), cobalt nitrate hexahydrate ($Co(NO_3)_2·6H_2O$, 99%), sodium molybdate dihydrate ($NaMoO_4·H_2O$, 99%) and potassium hydroxide (KOH, AR) were obtained from Aladdin Industrial Corporation, China. And acetone (AR), ethanol (AR) and hydrochloric acid (HCl) were purchased from Sinopharm Chemical Reagent Co., Ltd, China. All chemicals and solvents used in the experiment were not further purified.

1.2 Preparation of $Co_{11}(HPO_3)_8(OH)_6$ NRs

The detail of $Co_{11}(HPO_3)_8(OH)_6$ growth process has been reported by our previous investigation[1]. In a typical synthesis process, the 30 mL solution containing 0.098 g $Co(NO_3)_2·6H_2O$ and 0.159 g $NaH_2PO_2·H_2O$ was stirred for 30 min, then the mixture was poured into the vessel with a piece of nickel foam (NF, 2×2.2 cm^2) that was pre-treated with ethanol, HCl and acetone. Subsequently, the solution was heated to 140 °C for 12 h. Finally, pink $Co_{11}(HPO_3)_8(OH)_6$ on NF was obtained after drying at 60 °C for 6 h. The mass loading of $Co_{11}(HPO_3)_8(OH)_6$ on NF is about 3.7 mg/cm^2.

1.3 Preparation of $Co_{11}(HPO_3)_8(OH)_6$@$CoMoO_4$ via hydrothermal method

$Co_{11}(HPO_3)_8(OH)_6$@$CoMoO_4$ was prepared by hydrothermal method as follows: First, the 15 mL solution containing 0.124 g $NaMoO_4·H_2O$ and 0.145 g $Co(NO_3)_2·6H_2O$ was prepared. After stirring for 30min, the solution was transferred to the reaction kettle included NF (2×2.2 cm^2) with $Co_{11}(HPO_3)_8(OH)_6$. Then the solution was heated at 120, 140 and 160 °C for 5 h, respectively. After that, the

samples were rinsed with ethanol and deionized water (DI), and dried at 60 °C for 6 h. Finally, the sample was calcined in muffle furnace at 400 °C with the heating rate of 2 °C/min for 2 h in air. The mass loading of $Co_{11}(HPO_3)_8(OH)_6$@$CoMoO_4$ is about 4.1 mg/cm^2. The synthesis method of $CoMoO_4$ is the same as above; the blank NF without $Co_{11}(HPO_3)_8(OH)_6$ was placed in the reaction kettle, which was the only difference.

1.4 Preparation of $Co_{11}(HPO_3)_8(OH)_6$@$CoMoO_4$ via reflux method

0.124 g $NaMoO_4 \cdot H_2O$ and 0.145 g $Co(NO_3)_2 \cdot 6H_2O$ were dissolved in 15 mL DI water, and stirred for 30 min. Then the solution and NF (2×2.2 cm^2) with $Co_{11}(HPO_3)_8(OH)_6$ were transferred to a three-mouth bottle, placed in an oil bath, and refluxed at 60 °C for 6 h under stirring. After the reflux, the NF with the as-prepared materials was took out and rinsed with water and ethanol three times. Finally, $Co_{11}(HPO_3)_8(OH)_6$ that coated by $CoMoO_4$ was obtained. The mass loading of active material is about 2.5 mg/cm^2. The synthesis method of $CoMoO_4$ was the same as above, the blank NF without $Co_{11}(HPO_3)_8(OH)_6$ was placed in the three-mouth bottle, which is the only difference.

1.5 Structure characterization

Powder X-ray diffraction (XRD, Rigaku MiniFlexII X-ray diffraction, 30 kV, 15 mA, $\lambda = 0.15418$ nm) test was performed on the samples and the data were compared with the standard cards in the JCPDS to determine the phase and analyze the crystallization. The morphology of the samples was characterized by a scanning electron microscope (SEM, Hitachi SU8010, 10.0 kV). The microstructure and lattice

fringes of the samples were characterized by high resolution transmission electron microscope (TEM, FEI Tecnai G2F20, 200kV). N_2 adsorption/desorption (TriStar II 3020) was measured at 77 K and the specific surface area, pore size distribution and pore volume of the samples were analyzed. The specific area surface was calculated using the Brunauer-Emmet-Teller (BET) method. The chemical composition and elemental valence states of the samples were analyzed by X-ray photoelectron spectroscopy (XPS, ESCALab 250X; Monochromatic Al Kα source, 1486.6 eV).

1.6 Electrochemical characterization

The electrochemical performance of the samples was estimated in 2 M KOH solution using the electrochemical workstation (VersaSTAT3). The three-electrode system was constructed using $Co_{11}(HPO_3)_8(OH)_6$@$CoMoO_4$ grown on the NF (1×1 cm^2) as the positive electrode, a platinum foil as the counter electrode and a Hg/HgO electrode as the reference electrode. Cyclic voltammetry test (CV) was carry out at a range of 0-0.7 V from 10-50 mV/s. Galvanostatic charge-discharge test (GCD) was carried out within the 0-0.5 V from 1-20 A/g. The electrochemical impedance spectroscopy (EIS) analysis was performed in a frequency range of 0.01 Hz-10^5 Hz, and the amplitude was 5 mV. The specific capacity (C, C/g), coulomb efficiency (η, %), specific energy (E, Wh/kg) and specific power (P, W/kg) can be calculated according to the formula[2-4]:

$$C = \frac{It_d}{m} \qquad \text{(S1)}$$

$$\eta = \frac{t_d}{t_c} \times 100\% \qquad \text{(S2)}$$

$$E = \frac{1}{2} C \Delta V \qquad \text{(S3)}$$

$$P = \frac{E}{\Delta t} \qquad \text{(S4)}$$

Where I, m, t_d, t_c and ΔV are current density (A/g), loading mass (mg), discharge time (s), charge time (s) and voltage window (V), respectively.

The scan rate has a great influence on the response current during the CV test. In general, the formulas (S5) and (S6) that obeyed the powers law can illustrate the relationship between the current density and the scan rate[5, 6]:

$$i = av^b \qquad \text{(S5)}$$

$$\log(i) = \text{blog}(v) + \log(a) \qquad \text{(S6)}$$

Where i represents current density (A/g); v represents the scan rate (mV/s); a and b are constants. Among them, the b-valued is connected to the electrochemical process. If b=0.5, the electrochemical reaction is a diffusion-controlled (battery-type) process, whereas b=1 indicates surface-controlled (capacitive) process[7].

The capacitive contribution is analyzed according to the following formula[8]:

$$i = k_1 v + k_2 v^{1/2} \qquad \text{(S7)}$$

Where $k_1 v$ is surface-controlled process and $k_2 v^{1/2}$ is diffusion-controlled reaction.

2. Figures and Tables

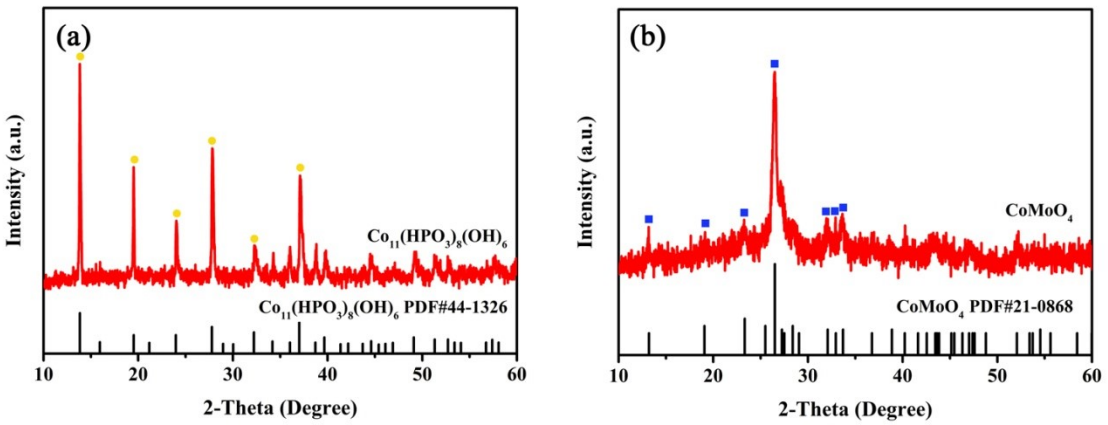

Fig. S1 XRD patterns: (a) $Co_{11}(HPO_3)_8(OH)_6$; (b) $CoMoO_4$–H.

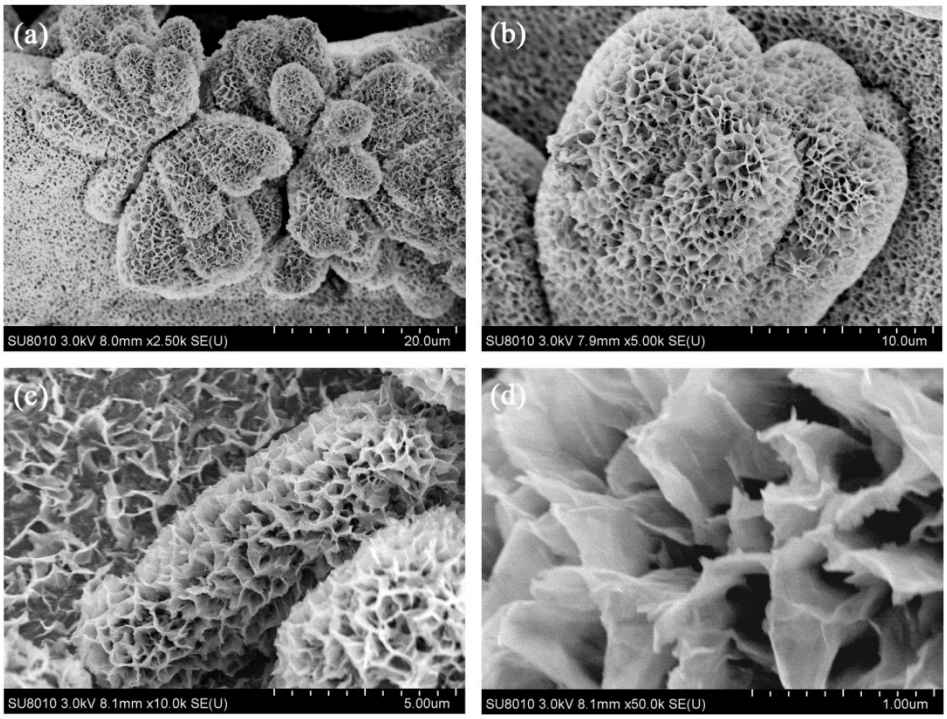

Figure S2 SEM of $Co_{11}(HPO_3)_8(OH)_6$@$CoMoO_4$–H at different temperatures: (a–b) 120 ℃ and (c–d)160 ℃.

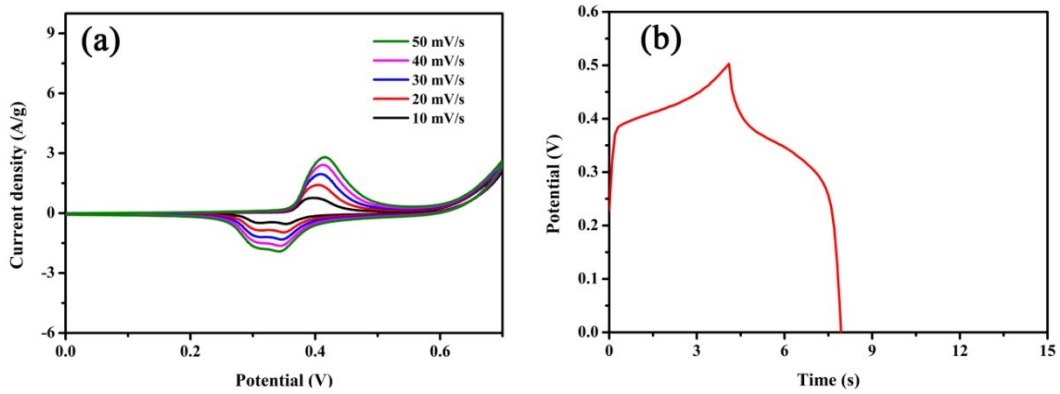

Figure S3 The electrochemical performance of Ni foam: (a) CV curves at 10–50 mV/s and (b) GCD curves at 1 A/g.

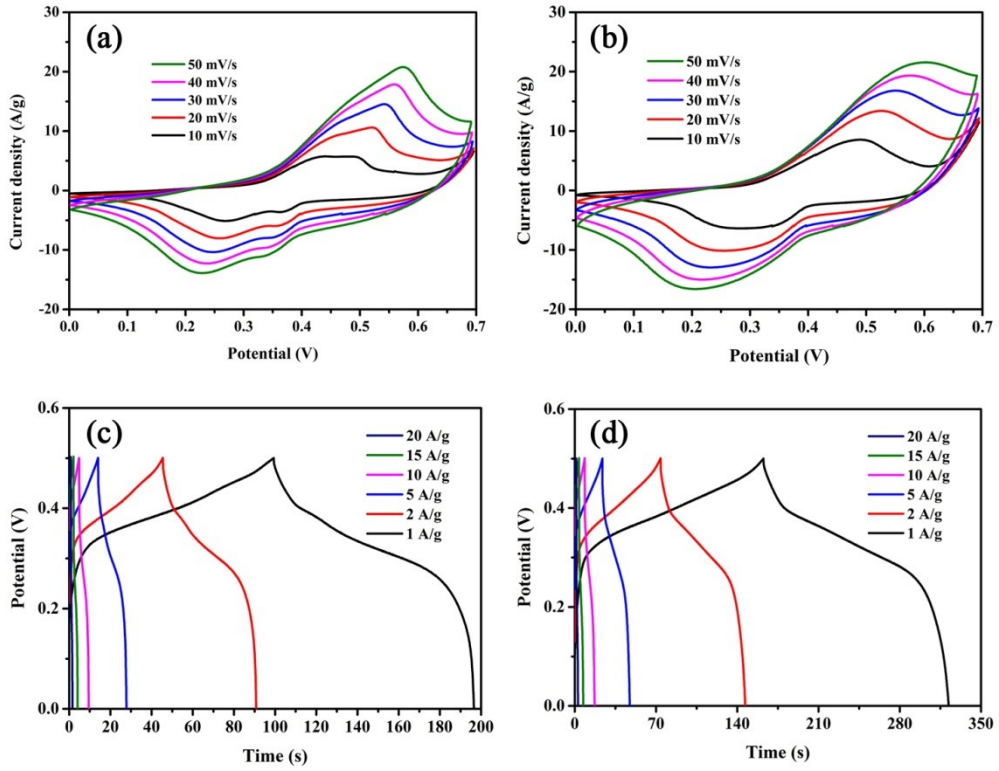

Figure S4 The CV curves at different scan rates and GCD curves at various current densities of (a and c) $Co_{11}(HPO_3)_8(OH)_6$; (b and d) $CoMoO_4$–H.

Table S1 The specific capacities of $Co_{11}(HPO_3)_8(OH)_6$, $CoMoO_4$–H and $Co_{11}(HPO_3)_8(OH)_6$@$CoMoO_4$–H and –R at different current densities.

Samples		Specific capacities (C/g)					
		1 A/g	2 A/g	5 A/g	10 A/g	15 A/g	20 A/g
$Co_{11}(HPO_3)_8(OH)_6$		97.3	90.8	69.0	48.0	30.0	16.0
$CoMoO_4$–H		159.7	146.0	118.0	85.0	55.5	28.0
$Co_{11}(HPO_3)_8(OH)_6$@$CoMoO_4$–H	120 °C	247.0	221.2	182.5	146.0	115.5	88.0
	140 °C	495.1	447.0	371.0	294.0	238.5	186.0
	160 °C	392.0	350.6	278.5	209.0	156.0	104.0
$Co_{11}(HPO_3)_8(OH)_6$@$CoMoO_4$–R	60 °C	837.1	744.2	586.0	442.0	351.0	302.0

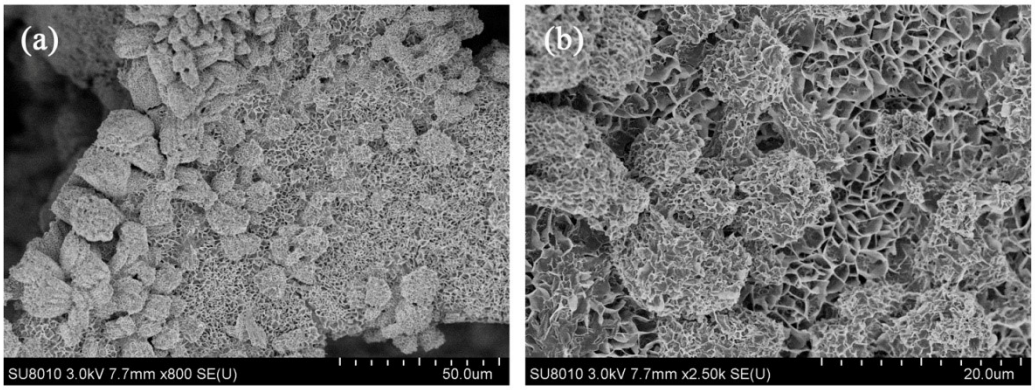

Fig. S5 SEM images of $Co_{11}(HPO_3)_8(OH)_6$@$CoMoO_4$–H after 4000 charge/discharge cycles.

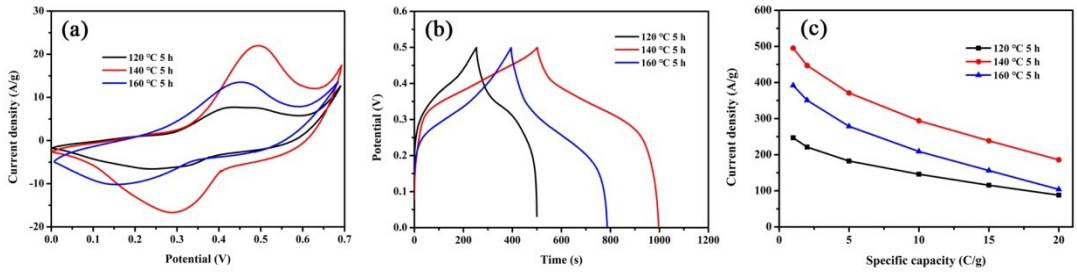

Fig. S6 The electrochemical performance of $Co_{11}(HPO_3)_8(OH)_6$@$CoMoO_4$–H obtained at 120, 140 and 160 °C: (a) CV curves at 10 mV/s; (b) GCD curves at 1 A/g; (c) the specific capacities at 1–20 A/g.

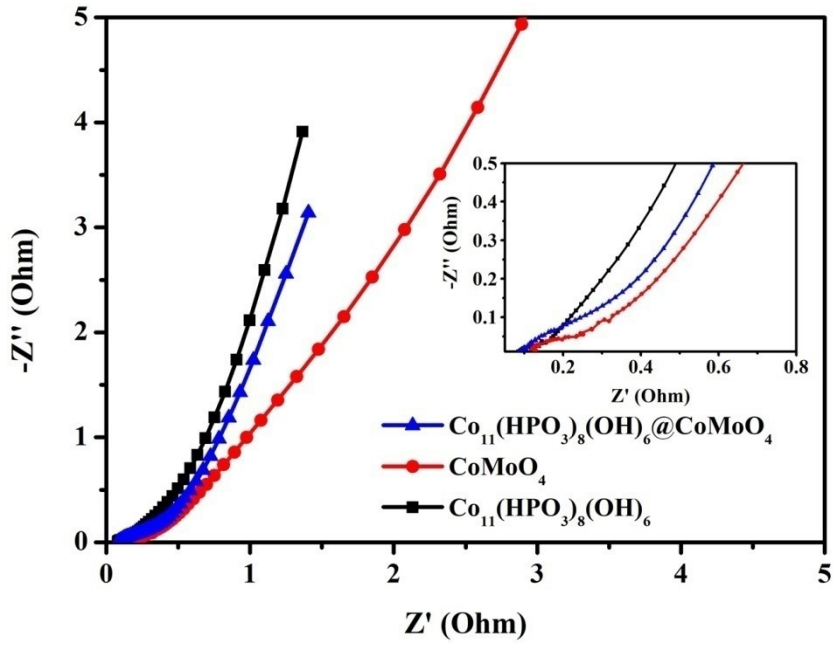

Fig. S7 The Nyquist plots of $Co_{11}(HPO_3)_8(OH)_6$, $CoMoO_4$–H, and $Co_{11}(HPO_3)_8(OH)_6$@$CoMoO_4$–H.

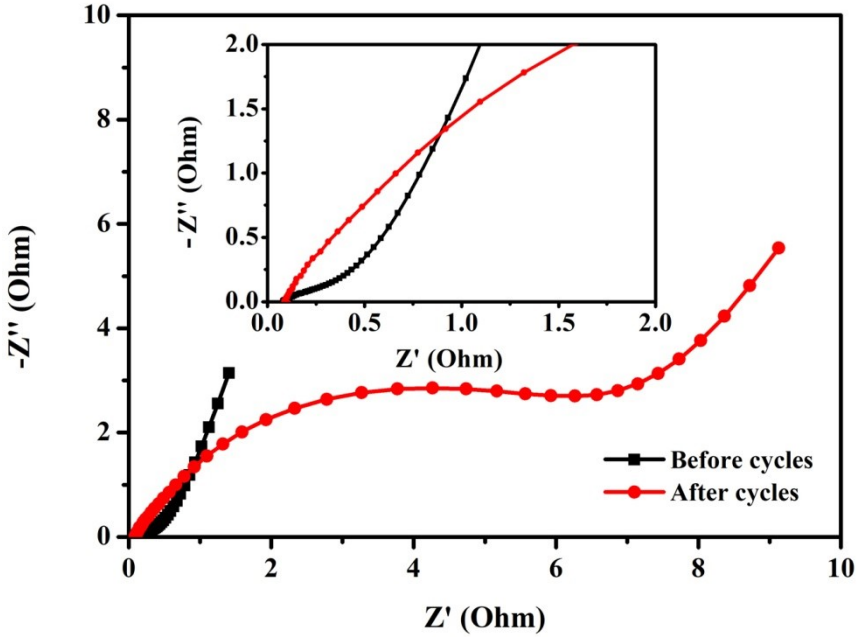

Fig. S8 The Nyquist plots of $Co_{11}(HPO_3)_8(OH)_6$@$CoMoO_4$–H before and after 4000 cycles.

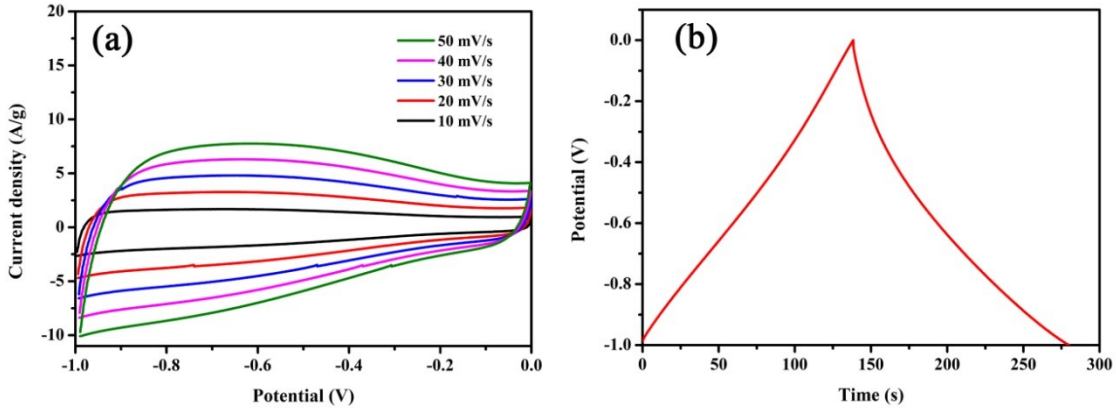

Fig. S9 The electrochemical performance of AC: (a) CV curves at 10-50 mV/s and (b) GCD curves at 1 A/g.

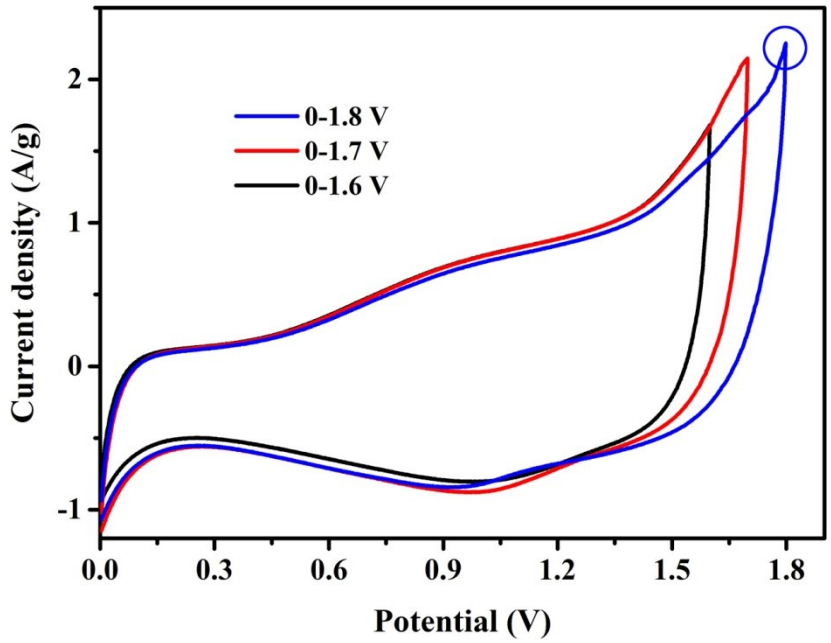

Fig. S10 The CV curves of the CHPO@CMO-H //AC HSC device under different operating voltage windows.

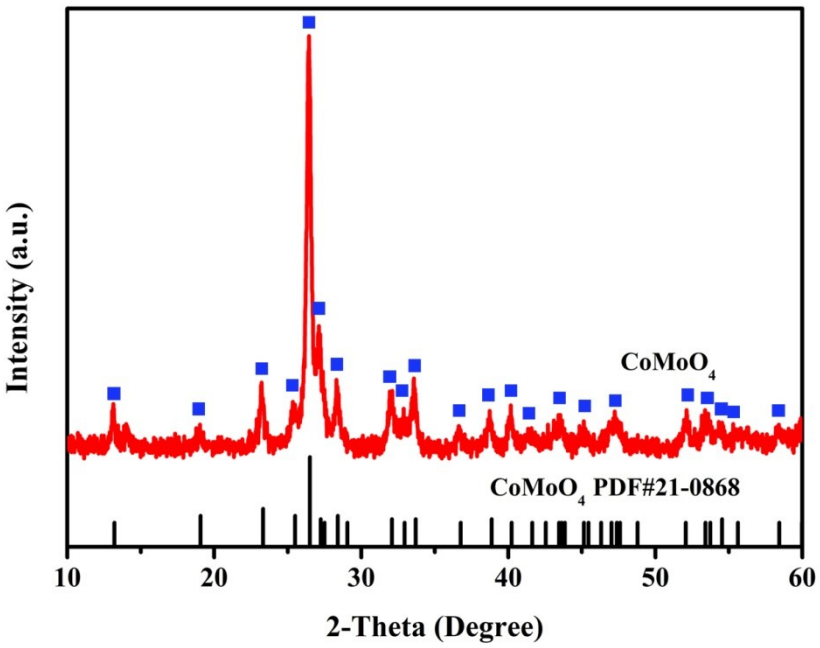

Fig. S11 XRD patterns of $CoMoO_4$–R.

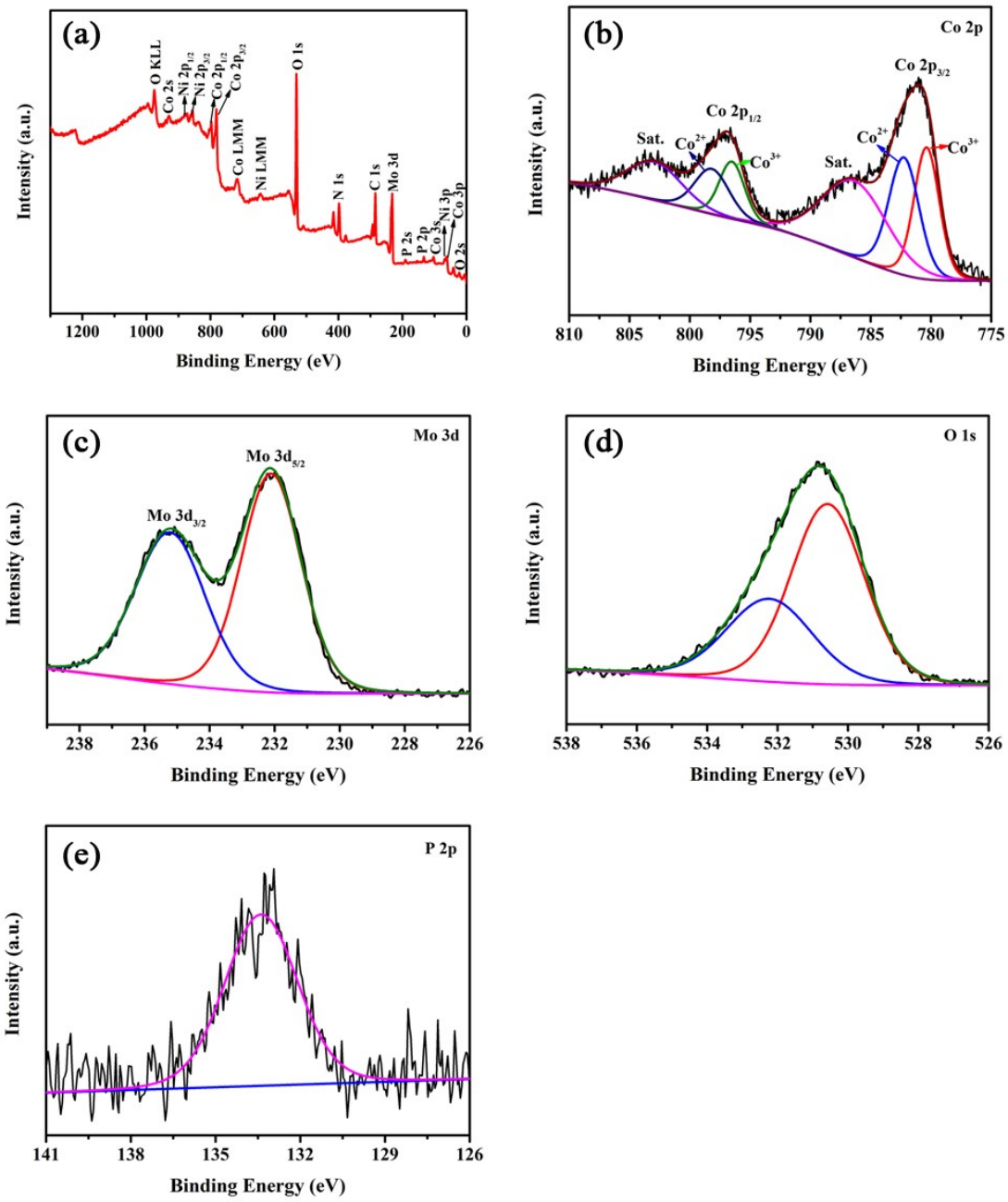

Fig. S12 The XPS spectra of $Co_{11}(HPO_3)_8(OH)_6$@$CoMoO_4$–R: (a) Survey spectrum; (b) Co 2p; (c) Mo 3d; (d) O 1s and (e) P 2p.

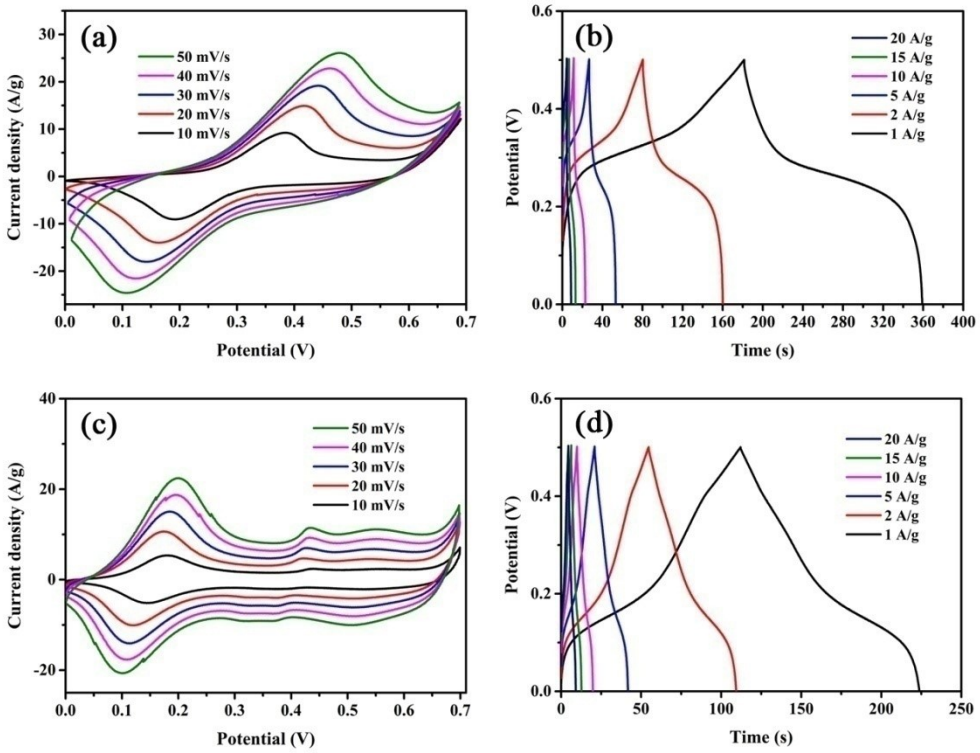

Fig. S13 The CV curves at 10–50 mV/s and GCD curves at 1–20 A/g: (a–b) $Co_{11}(HPO_3)_8(OH)_6$; (c–d) $CoMoO_4$–R.

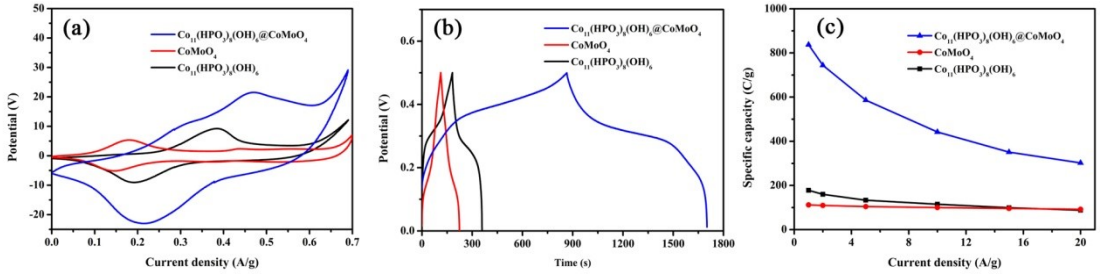

Fig. S14 The comparison of $Co_{11}(HPO_3)_8(OH)_6$, $CoMoO_4$ and $Co_{11}(HPO_3)_8(OH)_6$@$CoMoO_4$–R: (a) CV curves at 10 mV/s; (b) GCD curves at 1 A/g; (c) Specific capacities at 1–20 A/g.

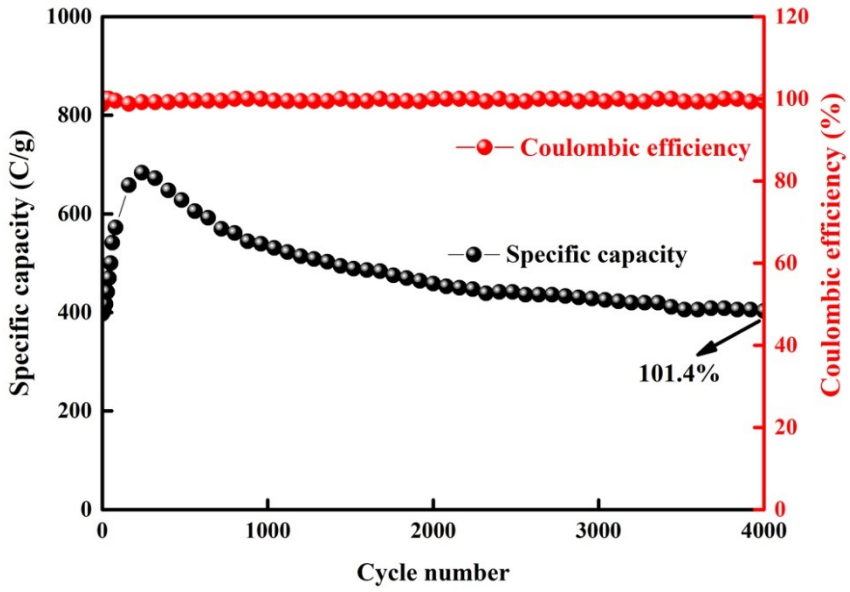

Fig. S15 Cyclic performance of $Co_{11}(HPO_3)_8(OH)_6$@$CoMoO_4$–R for 4000 cycles at 5 A/g.

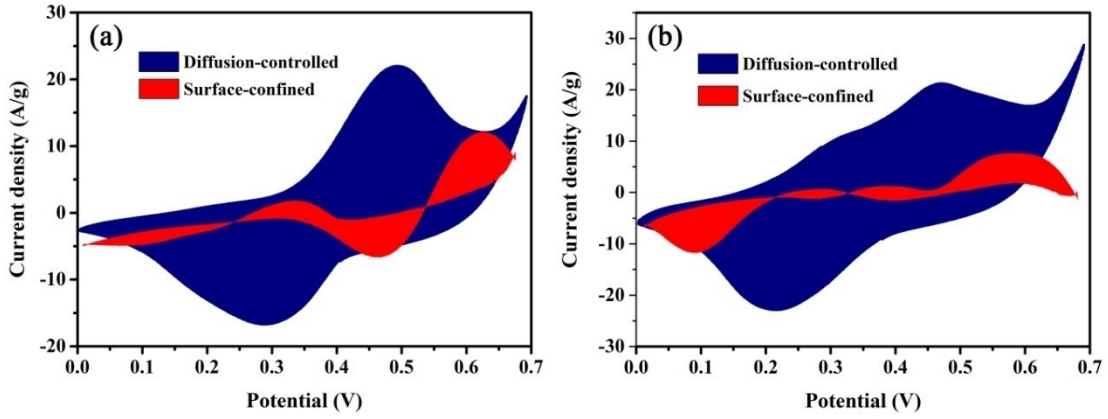

Fig. S16 Surface and diffusion–controlled contributions to charge storage of as–prepared samples at 10 mV/s. (a) $Co_{11}(HPO_3)_8(OH)_6$@$CoMoO_4$–H; (b) $Co_{11}(HPO_3)_8(OH)_6$@$CoMoO_4$–R.

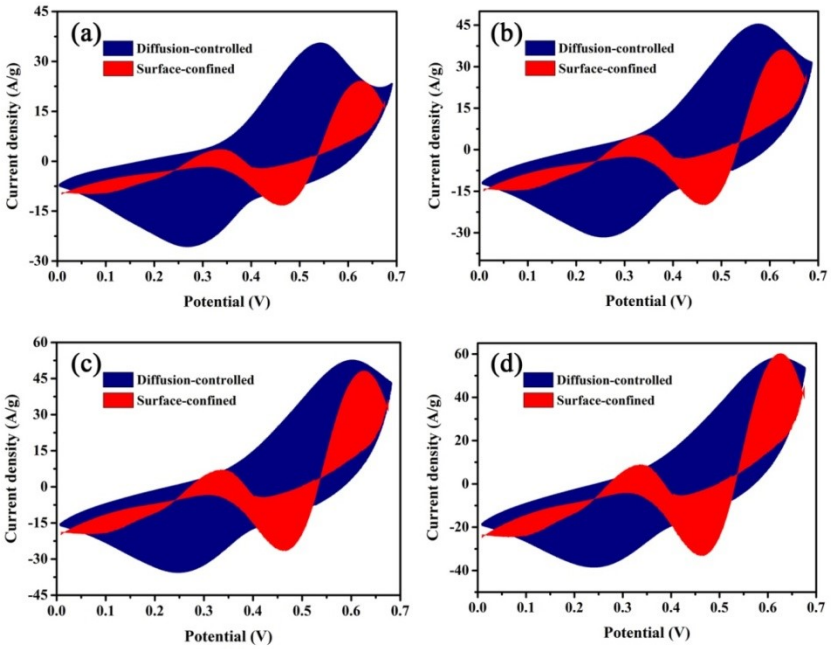

Fig. S17 Surface and diffusion–controlled contributions to charge storage of as–prepared $Co_{11}(HPO_3)_8(OH)_6$@$CoMoO_4$–H at different scan rates: (a) 20 mV/s; (b) 30 mV/s; (c) 40 mV/s; (d) 50 mV/s.

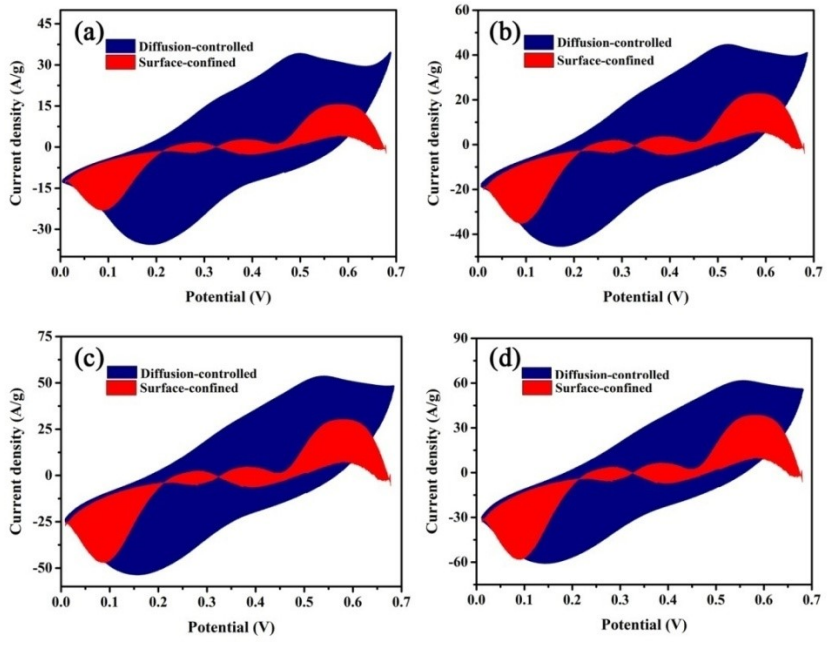

Fig. S18 Surface and diffusion–controlled contributions to charge storage of as-prepared $Co_{11}(HPO_3)_8(OH)_6$@$CoMoO_4$–R at different scan rates: (a) 20 mV/s; (b) 30 mV/s; (c) 40 mV/s; (d) 50 mV/s.

Table S2 Comparison of the specific energy and power of different devices assembled in our work and by some recent literatures.

Asymmetric supercapacitor	Energy density (Wh/kg)	Corresponding power density (W/kg)	references
$ZnCo_2O_4//Ni_xCo_{2x}(OH)_{6x}$	26.2	511.8	9
$Co_3(PO_4)_2$	26.66	750	10
$NiCo(PO_4)_3$/GF	34.8	377	11
$NaNi_{0.33}Co_{0.67}PO_4 \cdot H_2O$	29.85	374.95	12
$Mn_3(PO_4)_2$/GF	7.6	360	13
$Co_{11}(HPO_3)_8(OH)_6$	14.5	799.4	1
CHPO@CMO-H	**23.84**	**849.9**	**This work**
CHPO@CMO-R	**38.4**	**850.7**	**This work**

3. References

1. Y. Tian, X. Lian, Y. Wu, W. Guo, S. Wang, *CrystEngComm*, 2020, **22**, 5218-5225.

2. T. Shinomiya, V. Gupta, N. Miura, *Electrochim. Acta*, 2006, **51**, 4412–4419.

3. S. Tripathi, A. Kumar, S. Hashmi, *Solid State Ionics*, 2006, **177**, 2979-2985.

4. L. L. Zhang, X. S. Zhao, *Chem*. *Soc*. *Rev*., 2009, **38**, 2520-2531.

5. John Wang; Julien Polleux; James Lim; B. Dunn, *J. Phys. Chem. C*, 2007, **111**, 14925-14931.

6. V. Augustyn, J. Come, M. A. Lowe, J. W. Kim, P. L. Taberna, S. H. Tolbert, H. D. Abruna, P. Simon, B. Dunn, *Nat. Mater.,* 2013, **12**, 518-522.

7. P. Simon, Y. Gogotsi, B. Dunn, *Science* 2014, **343**, 1210–1211. .

8. Y. Yan, B. Hao, D. Wang, G. Chen, E. Markweg, A. Albrecht, P. Schaaf, *J. Mater. Chem. A,* 2013,**1**, 14507-14513.

9. W. Fu, Y. Wang, W. Han, Z. Zhang, H. Zha and E. Xie, *J. Mater. Chem. A*,

2016, **4**, 173-182.

10. K. V. Sankar, S. C. Lee, Y. Seo, C. Ray, S. Liu, A. Kundu and S. C. Jun, *J. Power Sources*, 2018, **373**, 211-219.

11. A. A. Mirghni, K. O. Oyedotun, B. A. Mahmoud, A. Bello, S. C. Ray and N. Manyala, *Compos. Part B-Eng.*, 2019, **174**, 106953.

12. M. Liu, N. Shang, X. Zhang, S. Gao, C. Wang and Z. Wang, *J. Alloy. Compd.*, 2019, **791**, 929-935.

13. A. A. Mirghni, M. J. Madito, T. M. Masikhwa, K. O. Oyedotun, A. Bello and N. Manyala, *J. Colloid Interf. Sci.*, 2017, **494**, 325-337.